3D spheroid model of adipose-derived stem cell and breast cancer cell co-culture for mimicking cell migration and the cancer environment

Dongwoo Kim
Seoul National University
Changheon Kim
Seoul National University
Chaewon Bae
Seoul National University
Changgi Hong
Seoul National University
Gyubok Lee
Seoul National University
Suhyun Ryu
Seoul National University
Yejin Lee
Seoul National University
Boa Song
THEDONEE Inc
Kangwon Lee
Seoul National University
Min Hee Park (conomo0850@gmail.com)
THEDONEE Inc

Research Article

Keywords: breast cancer, adipose-derived stem cell, 3D spheroid, extracellular matrix, cell migration, cancer invasion

Posted Date: December 12th, 2023

DOI: https://doi.org/10.21203/rs.3.rs-3736468/v1

Additional Declarations: No competing interests reported.

Abstract

Traditional two-dimensional (2D) cell culture methodologies exhibit significant limitations, notably their failure to replicate the intricate three-dimensional (3D) milieu of human tissue architecture. This discrepancy has catalyzed the exploration of advanced drug screening platforms that more faithfully mimic the complex 3D biological environment. To this end, precision medicine research has increasingly used 3D *in vitro* models that emulate the tissue microenvironment of the human body. In this study, breast cancer cell lines (MDA-MB-231 and SK-BR-3) were co-cultured with adipose-derived stem cells (ADSCs), mimicking the in vitro 3D tumor microenvironment with the multicellular and heterogeneous nature of solid tumors compared to a 2D cancer cell only system. Additionally, collagen type I was used to replicate the microenvironment within a 3D spheroid platform, enhancing the accuracy of the platform in mimicking human tissue characteristics. Significantly, the interactions between the ADSCs and two breast cancer lines markedly influenced factors such as cell elongation, molecular expression, migration patterns, and drug sensitivity. The integration of ADSCs was pivotal in simulating the cancer microenvironment, highlighting that even within the same cancer cell line, varying microenvironmental contexts can lead to vastly different experimental results. Thus, this study provides insights into the role of factors such as cellular substrates and stem cells in simulating a 3D tumor microenvironment more akin to the human body when constructing a 3D *in vitro* system based on breast cancer cells.

Introduction

Breast cancer remains a predominant malignancy among women globally and continues to pose a substantial health challenge. Conventional oncological therapies, including chemotherapy and radiotherapy, have demonstrated effectiveness in managing breast cancer; however, their associated adverse effects, such as anemia and thrombocytopenia, are profound [1, 2]. Consequently, there is an increasing focus among researchers on the development of drug screening systems that emulate the microenvironment of the human body. This approach is aimed at facilitating precision medicine, which is customized to align with the specific physiological conditions of a patient's body [3–5]. A promising approach for simulating the human microenvironment at the *in vitro* level involves the development of three-dimensional (3D) spheroids. These 3D spheroids, characterized by their 3D multicellular structure, closely replicate *in vivo* cellular responses and interactions, and are currently the subject of intensive research. [6] Their ease of resizing and reproducibility render 3D spheroids particularly suitable for high-content screening applications [7, 8].

Establishing an environment that closely resembles human physiology is essential for enhancing the precision of clinical drug screening. To this end, selecting an appropriate extracellular matrix (ECM) capable of accurately replicating the targeted disease environment, along with a suitable cell source, is critical. The ECM is integral to the structural integrity of the human body, serving as a reservoir for growth factors and cells, and has a pivotal role in cellular functions and interactions. [9–11] ECM proteins and components significantly impact cell signaling, migration, and trans-differentiation. Among various ECM constituents, collagen is the most abundantly distributed in the human body and has a crucial role in cell survival, cell-matrix interactions, and the transport of cell signaling molecules. This prominence underscores the vital function of collagen in maintaining cellular homeostasis and facilitating key physiological processes. [12, 13] The natural polymer properties of collagen make it highly suitable for utilization as a hydrogel and as an essential element in the construction of 3D *in vitro* platforms. Furthermore, the role of collagen in facilitating angiogenesis positions it as a critical factor in the evaluation of drug efficacy and toxicity in preclinical testing. [14] Therefore, the incorporation of collagen into 3D in vitro models significantly enhances the accuracy of these models by more closely mimicking the microenvironment of the human body.

Multicellular tumor spheroids are currently the subject of active research, focusing on how to effectively manipulate and control the 3D microenvironment. [15, 16] Considering that diverse cell types have interactive roles in the mechanisms of cancer development and progression, the incorporation of co-culture systems is essential in the design of *in vitro* models. In an actual physiological context, cancer growth involves not only isolated cancer cells but a complex interplay with other cell types such as fibroblasts and stem cells. This complexity must be accurately replicated in in vitro models to better understand and target the multifaceted nature of cancer. [17] Among the various cell types involved in cancer dynamics, adipose-derived stem cells (ADSCs) have a significant role in cancer migration and metastasis. ADSCs are gaining increasing importance in the context of breast cancer research due to their ability to secrete a range of growth factors that are instrumental in cancer growth and migration. [18] In context of tumor growth, the epithelial-to-mesenchymal transition (EMT) is a critical mechanism in cancer migration and metastasis. This process involves the transformation of tightly aligned epithelial cells into more mobile mesenchymal cells, which can freely move and spread. ADSCs have been reported to significantly influence the EMT and, consequently, cancer metastasis. As the EMT progresses, various molecular markers and structural proteins have pivotal roles. These include alpha-smooth muscle actin (α-SMA), CD44, N-cadherin, E-cadherin, and vimentin, along with junctional molecules such as fibronectin and integrins. These components are integral to the changes in cell adhesion, morphology, and motility associated with the EMT, thereby facilitating cancer cell migration and metastasis. [19–21]

This study established a 3D spheroid co-culture system comprising ADSCs and breast cancer cells (MBA-MB-231 and SK-BR-3) within a collagen matrix to investigate the distinct interactions between the ADSCs and cancer cells in both 2D and 3D cultures (Scheme 1). The focus was on examining critical factors in breast cancer growth and metastasis, including cell elongation, junction expression, and migration patterns in drug sensitivity. The developed 3D spheroid model, featuring a co-culture of breast cancer cells and ADSCs, provides a valuable framework for designing *in vitro* models of various carcinomas. Furthermore, these platforms offer a promising approach for future drug screening, potentially leading to more effective and targeted metastatic cancer therapies.

Experimental details

Cell culture conditions

Adipose-derived stem cells (ADSCs), the primary cells in this study, were obtained from Cell Bio (Seoul, Korea). The cell culture medium for the ADSCs was Dulbecco's Modified Eagle Medium (DMEM), supplemented with 1% penicillin-streptomycin (Welgene, Korea) and 10% FBS (Cellsera, NSW, Australia). The

breast cancer cell lines MDA-MB-231 and SK-BR-3 were acquired from the Korea Cell Line Bank (Seoul, Korea). Breast cancer cells were cultured using Roswell Park Memorial Institute medium (RPMI), supplemented with 1% penicillin–streptomycin (Welgene, Korea) and 10% FBS (Cellsera, NSW, Australia). The cell culture was maintained in an incubator at 37°C under a 5% CO_2 atmosphere.

Preparation of agarose gel plate and collagen matrix

The 3D spheroids were fabricated using an agarose gel (Sigma Aldrich, USA). First, after dissolving 2% agarose in Dulbecco's Phosphate-Buffered Saline (DPBS), 60 µL of agarose gel were dispensed into a 96-well plate. Thereafter, the agarose plate was incubated on a clean bench at room temperature for 30 minutes, followed by ultraviolet light disinfection for 30 minutes. Then, 5×10^4 breast cancer cells were added to the ADSCs at a 1:1 ratio, and after 48 hours, spheroids were formed spherically. To fabricate the collagen matrix, 110 µL of 2 mg/mL collagen type I were dispensed into each well of a 96-well plate. To neutralize the acidity, 1 N NaOH was added. Then, 80 µL of this mixture were dispensed into each well of the 96-well plate and cured at 37°C for 30 minutes.

Optimization of Morphological Stability in 3D Spheroids and Collagen gel transfer

3D Spheroids were formed in the 1×10^4, 1.5×10^4, 2×10^4, and 5×10^4 breast cancer cells and ADSCs at a 1:1 ratio separately. Using the same process, we also tried spheroid formation with a 1%, 1.5%, and 2% agarose gel (Sigma Aldrich, USA) and the 5×10^4 breast cancer cell line and ADSCs. Thereafter, the stability of the spheroid shape was observed using a bright-field microscope. (Carl Zeiss, Oberkochen, Germany) The 3D spheroid was extracted using a 1000 µL tip and then transferred to a collagen matrix.

Cell viability assay

Cell viability within the 3D spheroids was assessed using a Live/Dead Kit (Invitrogen, USA). Viability measurements were conducted at two time intervals, 24 and 48 hours post-formation of the 3D spheroids. The groups evaluated included the ADSCs, MDA-MB-231, and ADSCs and MDA-MB-231 (AD), and ADSCs and SK-BR-3 (AS) groups. For the viability assay, the 3D spheroids were treated with 2 µM calcein AM and 4 µM ethidium homodimer-1 (EthD-1) for 30 minutes. Following the treatment, the spheroids were washed 2–3 times with sterile phosphate-buffered saline (PBS) to remove excess dye. Subsequently, fluorescence imaging was performed to evaluate cell viability.

Immunofluorescence staining

The expression levels of the cells were determined using immunofluorescence staining. Initially, the cells were fixed with 4% paraformaldehyde (Dana Korea, Korea) for 30 minutes. This was followed by permeabilization using Triton-X for 10 minutes at room temperature. For staining, the cells were incubated with the primary antibody for 2 hours and then with the secondary antibody overnight at 4°C. Finally, the cells were stained with DAPI for 15 minutes at room temperature to visualize the nuclei.

Fluorescence imaging for analysis of cell migration within a 3D spheroid embedded in a collagen matrix

Cell migration was monitored using Green Cell Tracker (Invitrogen, USA) for the breast cancer cells and Vybrant dye (Invitrogen, USA) for the ADSCs. For the breast cancer cells, 500 µL of 10 mM Green CMFDA Dye were added to the breast cancer cell pellet, followed by incubation of $1x10^5$ cells at room temperature for 30 minutes. For the ADSCs, Vybrant dye was prepared by adding 5 µL of cell-labeling solution to 1 mL based on $1x10^5$ cells, and the cells were incubated for 15 minutes.

Real-Time Quantitative Polymerase Chain Reaction (RT-qPCR)

The gene expression rate of the cells was confirmed by quantitative real-time polymerase chain reaction (qPCR). For the qPCR, Thermofisher Quantastudio 5 (Applied Biosystems, USA) was used. First, TRIzol for 5 minutes was used to extract isolated cellular ribonucleic acid (RNA), and the RNA was purified using chloroform, isopropyl alcohol, and ethanol consecutively. Then, after quantifying the nucleic acid using NanoDrop, we synthesized cDNA with the SuperScript™ VILO™ Master Mix (Invitrogen, USA) based on 1 µg, followed by a termination process at 5 minutes at 85°C and then 99 minutes at 42°C. The synthesized cDNA was stored in a − 80°C deep freezer. After a denaturation process of 95°C for 10 minutes, the cDNA was used with the target primer and quantiNova SYBR Green PCR Kit in the qPCR. The primer sequence is described in Additional file 1.

Doxorubicin treatment and migration assay

In the 3D spheroid model, AD and AS groups, formed using the agarose gel, were embedded in a 96-well plate coated with 2% collagen matrix. These spheroids underwent treatment with doxorubicin obtained from Sigma Aldrich, USA. The drug was diluted in a 1:1 mixture of Dulbecco's Modified Eagle Medium (DMEM) and Roswell Park Memorial Institute (RPMI) media prepared under serum-free conditions. Concentrations of 1 µM and 10 µM doxorubicin were administered to the AD and AS groups, respectively. Post-treatment, cell migration was evaluated and compared to a control group using bright-field microscopy.

Scanning electron microscopy (SEM) imaging

After the 3D co-culture involving the ADSCs, MDA-MB-231, and SK-BR-3, the resulting 3D spheroids were prepared for observation under scanning electron microscopy. The spheroids were fixed at 4°C using a 2.5% glutaraldehyde solution. Subsequently, they were treated with 2% osmium tetroxide (OsO_4) for 2 hours at the same temperature. Following this, the spheroids were washed several times with deionized water to remove any residual staining agents. The spheroids were then dried using hexamethyldisilazane and placed in a vacuum chamber for 24 hours. Finally, scanning electron microscopy images were captured using an FE-SEM Hitachi S 4100 (Hitachi, Japan).

Statistical analysis

All data are expressed as the mean ± standard deviation, and each experiment was performed three times. Data from the in vitro experiments were analyzed using a one-way analysis of variance (ANOVA), followed by Tukey's post hoc test. The statistical significance was *$p < 0.05$, **$p < 0.01$, and ***$p < 0.001$.

Results

Verifying interaction with Breast cancer cells and ADSCs through a cell elongation test in a collagen matrix

This study underscores the critical role of cell elongation and morphological changes in the migration, growth, and metastasis of cancer cells, as highlighted in previous research [22, 23]. Specifically, ADSCs have been reported to facilitate the EMT in various cancers, including lung and pancreatic cancers [24, 25]. To explore the morphological or structural changes in cells and to elucidate the interaction between ADSCs and breast cancer cells, this study involved culturing ADSCs with breast cancer cell lines MDA-MB-231 and SK-BR-3 on a plate with a 2 mg/mL collagen concentration, thereby establishing an ECM environment (Fig. 1.A). Post co-culturing with ADSCs, the degree of elongation was measured in fluorescently stained breast cancer cells (Fig. 1.B).

$$\mathrm{Elongation(a.u.)} = \frac{\mathrm{LongAxis}}{\mathrm{ShortAxis}}$$

The results indicate that the ADSCs and MDA-MB-231 (AD) group exhibited an elongation value ranging from 2 to 6, while the ADSCs and SK-BR-3 (AS) group showed a lower elongation value, converging to 1. This result indicated a significant difference in the elongation value of the AD group but not in the AS group. The breast cancer cell lines MDA-MB-231 and SK-BR-3 were selectively stained using CellTracker™ Green CMFDA dye and observed at 24 and 48 hours through bright-field microscopy, cell tracker, and merge imaging (Fig. 1.C). Furthermore, immunofluorescence staining was used to visualize intracellular microfilaments (e.g., F-actin) in the cytoskeleton of both breast cancer cells and ADSCs (Fig. 1.D). Notably, microfilament elongation was observed in the ADSCs only and the AD group but not in the breast cancer cells alone or the AS group.

These results suggest that ADSCs specifically influence the morphological changes in MDA-MB-231 cells, inducing them into an elongated form conducive to migration. In contrast, SK-BR-3 cells, despite being a breast cancer cell line, did not exhibit significant morphological changes in the presence of ADSCs. This differential response highlights the complexity of cell-cell interactions within the tumor microenvironment and underscores the need for tailored approaches in cancer *in vitro* modeling.

Investigating the Impact of ADSC Co-Culture on Cancer Migration, Growth, and Metastasis

In the study of cancer migration, growth, and metastasis, a key observation was the increased expression of cell surface adhesion factors and the transformation of intercellular junctions from tight to more permissive forms, facilitating cell migration. Fibronectin, a crucial mediator of communication between the ECM and cells, and integrin, which mediates interactions between the cytoskeleton and ECM, are central to these processes. [26, 27] Through immunofluorescence imaging, the study detected the presence of E-cadherin, a protein known to promote cancer migration and metastasis. Additionally, RT-qPCR was used to evaluate gene expression differences between 2D co-cultures of ADSCs and breast cancer cells and breast cancer cell monocultures, particularly focusing on the EMT, a key aspect of the metastatic environment, and the growth and migration of cancer cells.

Immunofluorescence imaging showed that in the ADSCs monocultures, fibronectin was expressed, but integrin and E-cadherin showed no fluorescence, suggesting that ADSCs are in a mesenchymal state conducive to migration. In contrast, MDA-MB-231 and SK-BR-3 cancer cell monocultures expressed both fibronectin and integrin, indicating active interaction with the ECM, but also exhibited high E-cadherin expression, suggesting that these cells were in an epithelial state less prone to migration. The co-culture groups (AD and AS groups) showed high expression of fibronectin and integrin but no E-cadherin expression, indicating a mesenchymal state more conducive to migration and invasion. This suggests that using a single cancer cell line for in vitro modeling may be insufficient to simulate the complex processes of migration and invasion critical to cancer metastasis.

Furthermore, RT-qPCR analysis supported these findings. It showed that in the ADSCs and breast cancer cell co-cultures, there was a significant increase in the expression levels of transforming growth factor-beta (TGF-β) and nuclear factor-κB (NF-κB), both of which are crucial in promoting cancer growth and are upregulated during cancer metastasis. Compared to the monocultures, the co-culture increased TGF-β by 1.25 to 9.11 times and NF-κB by 1.32 to 8.01 times, indicating a more cancer-like environment in the co-culture. These results demonstrate that an *in vitro* cancer model relying solely on a breast cancer cell line may not adequately replicate the complex tumor microenvironment. The co-culture of a breast cancer line with ADSCs, forming a multicellular model, showed an increase in tumor growth and regulation factors, more accurately mimicking a cancer-like environment. Thus, the weak intercellular junctions and elongated morphology of the ADSCs significantly contributed to enhanced cancer migration and growth.

Optimization of 3D Spheroid using Adipose-derived stem cells and Breast cancer cells and viability test

In the pursuit of establishing a 3D in vitro environment that closely mimics the tissue microenvironment of the human body for cancer research, this study focused on the utilization of ADSCs and breast cancer cell lines including MDA-MB-231 and SK-BR-3. The methodology involved dispensing these cells onto a plate coated with agarose gel, allowing for self-organization for two days (Fig. 3.A). Initially, different concentrations of agarose gel (1%, 1.5%, and 2%) were tested with ADSCs only, AS, and SK-BR-3 only groups to optimize the 3D spheroid formation (Fig. S1). The SK-BR-3 only group was dispensed with a 2% agarose gel concentration to achieve the most stable spheroid formation. When varying numbers of the ADSCs (1×10^4, 2×10^4, and 5×10^4 cells) were dispensed with a 2% agarose concentration, the highest cell count (5×10^4) formed the most stable spherical shape (Fig. S1).

It was observed that while the ADSCs only group formed a 3D spheroid effectively, the MDA-MB-231 only and SK-BR-3 only groups did not establish the 3D spheroid, likely due to a lower intercellular force. However, in the AD, and AS groups, spheroid formation was successful. A live/dead assay was conducted to

assess intracellular apoptosis during the formation of the 3D spheroid (Fig. 3.B),which did not show any significant cell death signals in all groups. Moreover, in both the AD and AS groups, the formation of ECM fibers on the surface of the 3D co-cultured spheroids was observed through scanning electron microscopy (Fig. 3.C). These results indicate that ADSCs not only facilitate the formation and self-organization of 3D spheroids but also have a significant role in promoting cell migration and the EMT, as seen in Figs. 1 and 2. The results underscore the crucial role of ADSCs in the formation of a 3D spheroid model, suggesting their potential as a key component in developing more accurate and representative in vitro models for breast cancer research.

Evaluating Cancer Invasiveness in 3D Spheroid Models: Insights into Migration Patterns and Gene Expression

The degree of migration in 3D environments is a critical aspect of assessing cancer invasiveness. [28] To evaluate the invasiveness of the 3D spheroid model, the migration distances of the ADSCs only, AD, and AS groups were measured using bright-field microscopy for 48 hours (Fig. 4.A). The results showed the AD group exhibited the longest migration distance, reaching up to 902 μm, followed by the ADSC only group at 503 μm, and the AS group at 109 μm. This result suggests that the AD group easily migrated more in three dimensions compared with the AS and the ADSC only groups.

Additionally, fluorescence imaging was used to track the individual migration patterns of ADSCs, MDA-MB-231, and SK-BR-3 in the 3D matrix (Fig. 4.C). The migration and aggregation patterns were markedly different between the AD and AS groups. In the AD group, ADSCs and MDA-MB-231 cells formed a uniformly mixed alloy spheroid within 1 hour of co-culture and continued to interact and migrate even after 48 hours. Conversely, in the AS group, a heterogeneous spheroid with a core–shell structure was formed after 1 hour. The MDA-MB-231 only group showed weak aggregation, while at 48 hours, the ADSC only group migrated in a 3D pattern, unlike the SK-BR-3 only group. These observations indicate that even within the same breast cancer line, the pattern of 3D spheroid formation can vary significantly when ADSCs are co-cultured with breast cancer cells, with MDA-MB-231 showing a stronger interaction with ADSCs compared to SK-BR-3.

Further analysis was conducted using RT-qPCR to compare gene expression levels in co-cultures of the breast cancer cell lines and ADSCs (Fig. 4.D). This comparison focused on the gene expression rates of integrin and α-SMA (a cell adhesion protein influencing cell migration), vimentin (an EMT marker), and CD44v6 (a cancer progression marker). The AD group exhibited higher gene expression levels of integrin, α-SMA, vimentin, and CD44v6 (2.21, 3.07, 2.72, and 4.77 times higher, respectively) compared with the AS group. Therefore, the 3D spheroid model of the AD group more effectively mimics cancer cell migration, invasion, metastatic mesenchymal form, and the cancer environment compared to the AS group. These findings highlight the importance of the tumor microenvironment and cell-cell interactions in cancer progression and underscore the potential of 3D spheroid models in cancer research.

Assessing Drug Efficacy in 3D Spheroids: Variability in Cancer Cell Response to Doxorubicin Treatment

The exploration of drug efficacy using 3D spheroids is a significant step in understanding how different cancer cell lines respond to chemotherapy. The invasion distance was investigated by measuring the cell migration distance after treatment with doxorubicin, a well-known anticancer drug, in the AD and AS groups. The objective of this study was to observe the reaction between anti-cancer drugs and these groups to doxorubicin treatment. The AD and AS groups were treated with doxorubicin at concentrations of 1 and 10 μM, respectively. The cell migration distance was then measured at various time points, ranging from 1 to 48 hours post-treatment. The results showed a significant impact of doxorubicin on cell migration. In the AD group treated with 10 μM doxorubicin, the migration distance decreased dramatically to 2.8 ± 0.4 μm compared to a distance of 53.3 ± 7 μm for the control group. In contrast, the AS group exhibited a decrease in migration to 9.1 ± 0.5 μm from the control's 22.2 ± 2 μm.

These results indicate that in the AD group, the migration was reduced by 94.5% compared to the control group, while in the AS group, the invasion distance was reduced by 57.4% compared to the control after doxorubicin treatment. This disparity in response to the same concentration of doxorubicin in the same 3D breast cancer model provides the importance of cell selection in modeling. The differences between the AD and AS groups could be attributed to the variations in their interactions with the ADSCs and the morphological changes occurring during the co-culture. In summary, this study highlights that even within the same type of breast cancer, the invasion distance after treatment with anticancer drugs can vary significantly depending on the cell line used. This emphasizes the complexity of cancer biology and the need for precise and tailored approaches in cancer treatment and drug efficacy studies.

Discussion

The incorporation of collagen in our 3D spheroid model represents a crucial advancement in cancer research, addressing the limitations of previous studies that largely neglected the complex interactions in a 3D microenvironment. [29, 30] This use of collagen in this study is not merely a methodological choice but a pivotal element that closely mimics the extracellular matrix ECM found in the cancer microenvironment, thereby providing a more accurate and relevant setting for understanding cancer progression. Collagen, a primary component of the ECM, has a vital role in cancer development and metastasis. [31, 32] Its presence in our 3D model is instrumental in studying the behaviors of breast cancer cells, specifically MDA-MB-231 and SK-BR-3, in response to ADSCs. Previous research, primarily based on 2D models, has been limited in replicating these critical ECM interactions, leading to a gap in our understanding of how the physical and biochemical properties of the ECM influence cancer cell behavior. [33] This research suggests the importance of collagen in modulating the behavior of breast cancer cells within a 3D environment. In Figure. 1A, the differential effects of the ADSCs on the morphology and migration of the MDA-MB-231 and SK-BR-3 cells, observed in the presence of collagen, highlight the dynamic interplay between cancer cells and their surrounding matrix.

There have been reports that ADSCs promote an inflammatory environment conducive to the growth of breast cancer cells [34], and increase drug resistance [35]. However, reports of ADSCs inducing morphological changes in breast cancer cells within a collagen matrix have been scarce. The significance of morphological changes in cancer cells can be attributed to the Epithelial-mesenchymal transition (EMT). This process involves cell adhesion factors such as fibronectin and integrin [36], EMT activation-related TGF-β [37], and cell survival factors like NF-κB [38], all of which were observed to increase when ADSCs

and breast cancer cells were co-cultured, as qualitatively and quantitatively seen in Fig. 2A and B. This interaction is crucial in determining the ability of cells to migrate, invade, and respond to treatments, which are key factors in cancer progression and metastasis.

The incorporation of collagen in our 3D spheroid model addresses a significant limitation in previous cancer research, which often neglected cellular migration and aggregation. While cell movement can be observed in a 2D environment using methods like the scratch assay, tracking this movement in a more realistic 3D human body environment is challenging. As in Fig. 4.A, we created spheroids and embedded them in a collagen matrix to observe cellular movement and aggregation in three dimensions. The AD group after one hour showed an alloy-type mixture of MDA-MB-231 and ADSCs, which then actively aggregated and migrated at 48 hours. In contrast, the AS group initially presented a core-shell type separation at one hour, followed by only ADSCs migrating at 48 hours. This finding is significant as it corroborates the morphological changes and gene expression variations observed in Figs. 1 and 2, suggesting that the AD group more closely resembles the cancer microenvironment, even in a three-dimensional context. Additionally, the relevance of collagen in our study extends to the realm of drug testing and therapy development. The differential responses to doxorubicin treatment in the 3D collagen-enriched environment compared to 2D cultures highlight the necessity of incorporating ECM components for accurate drug efficacy studies. In conclusion, this study not only bridges a significant gap in cancer research by using a collagen-enriched 3D spheroid model but also emphasizes the crucial role of ECM components, like collagen, in understanding the intricacies of cancer progression. The insights gained from this research pave the way for more sophisticated and accurate models in oncology, ultimately contributing to the development of more effective cancer treatments that consider the full spectrum of the tumor microenvironment.

Conclusion

In this study, the interaction between ADSCs and breast cancer cell lines (MDA-MB-231 and SK-BR-3) was investigated using a 3D spheroid platform. The results showed ADSCs significantly influence the morphological changes, migration, and invasion capabilities of MDA-MB-231 cells but not SK-BR-3 cells. Co-culturing with ADSCs led to increased cell elongation and a mesenchymal form conducive to migration. Gene expression analysis showed higher levels of factors promoting cancer growth and metastasis in the co-culture environment, indicating a more accurate cancer model. The study also demonstrated that the response to anticancer drugs varies significantly between different breast cancer cell lines when co-cultured with ADSCs. These results provide the importance of the tumor microenvironment in cancer progression and highlight the need for comprehensive in vitro models that incorporate cellular interactions for more effective cancer research and drug development.

Declarations

Ethics approval and consent to participate

Not applicable

Consent for publication

Not applicable

Availability of data and material

All date generated of analyzed during this study are included in this article.

Competing interests

The authors declare that they have no competing interests.

Funding

This work was supported by the National Research Foundation of Korea(NRF) grant funded by the Korea government(MSIT). (No. 2018R1C1B6002333 and 2021R1A2C2014268). The funding body played important role in the design of the study and collection, analysis, and interpretation of data and in writing the manuscript.

Author' contributions

DWK : conception and design, manuscript writing, experiment. CHK : Cell preparation protocol, CWB : Agarose and collagen substrate fabrication, CGH : Bio-imaging and data processing, GBL : data interpretation, SHR : Data processing and visualization, YJL : manuscript writing, BAS : data interpretation, KWL : supervision and editing , MHP : supervision the research and editing.

Acknowledgement

This work was in part supported by the Research Institute for Convergence Science.

Author details

[1]Department of Applied Bioengineering, Graduate School of Convergence Science and Technology, Seoul National University, Seoul, Korea. [2]Program in Nanoscience and Technology, Graduate School of Convergence Science and Technology, Seoul National University, Seouo, 08826, Republic [3]Research Institute for Convergence Science, 145, Gwanggyo-ro, Yeongtong-gu, Suwon-si, Gyeonggi-do, Republic of Korea. [4]THEDONEE Inc. Research Center, Seoul, Korea.

References

1. Parton M, Ring A (2016) Breast Cancer Survivorship: Consequences of early breast cancer and its treatment. 1st edn. Springer International Publishing : Imprint: Springer, Cham pp. 1 online resource (XV, 284 pages 18 illustrations, 13 illustrations in color
2. Rashid S, Saxena A, Rashid S (2023) Latest advances in diagnosis and treatment of women-associated cancers. First edition. edn. CRC Press, Boca Raton, FL pp. 1 online resource
3. Kurkuri M, Losic D, Uthappa UT, Jung H-Y (2023) Advanced porous biomaterials for drug delivery applications. CRC Press, Boca Raton, FL
4. Verma S, Verma S (2022) Advancements in controlled drug delivery systems. Medical Information Science Reference, Hershey, PA
5. Li J (2022) Biomaterials and materials for medicine: innovations in research, devices, and applications. Emerging materials and technologies, First edition. edn. CRC Press, Boca Raton, FL pp. 1 online resource
6. Das M, Santana MC, Barraque S, Cardenas J, Galindo JA, Cortes M, Ramos J, Prado AS, Castillo MT, Villar V, Vincent C, Justo E, Mendez M, Mera I, Pachon J, Perez K, Marin A, Murmu N, Biswas M, Ruiz M, Das JK (2021) 3D spheroid: A rapid drug screening model for epigenetic clinical targets against heterogenic cancer stem cells. Cancer Res 81
7. Wan X, Li ZH, Ye H, Cui ZF (2016) Three-dimensional perfused tumour spheroid model for anti-cancer drug screening. Biotechnol Lett 38:1389–1395. 10.1007/s10529-016-2035-1
8. Gorican L, Gole B, Potocnik U (2020) Head and Neck Cancer Stem Cell-Enriched Spheroid Model for Anticancer Compound Screening. Cells 9. doi: ARTN 170710.3390/cells9071707
9. Yadav S, Arya DK, Pandey P, Anand S, Gautam AK, Ranjan S, Saraf SA, Rajamanickam VM, Singh S, Chidambaram K, Alqahtani T, Rajinikanth PS (2022) ECM Mimicking Biodegradable Nanofibrous Scaffold Enriched with Curcumin/ZnO to Accelerate Diabetic Wound Healing via Multifunctional Bioactivity. Int J Nanomed 17:6843–6859. 10.2147/Ijn.S388264
10. Carpentier N, Campinoti S, Urbani L, Dubruel P, Van Vlierberghe S (2022) Development of ECM mimicking 3D-hydrogel scaffolds for liver tissue engineering. J Hepatol 77:S734–S735
11. Mukherjee A, Bravo-Cordero JJ (2023) Regulation of dormancy during tumor dissemination: the role of the ECM. Cancer Metastasis Rev. 10.1007/s10555-023-10094-2
12. Massimino LC, Martins VDA, Vulcani VAS, de Oliveira VL, Andreeta MB, Bonagamba TJ, Klingbeil MFG, Mathor MB, Plepis AMD (2020) Use of collagen and auricular cartilage in bioengineering: scaffolds for tissue regeneration. Cell Tissue Banking. 10.1007/s10561-020-09861-0
13. Smolar J, De Nardo D, Reichmann E, Gobet R, Eberli D, Horst M (2020) Detrusor bioengineering using a cell-enriched compressed collagen hydrogel. J Biomedical Mater Res Part B-Applied Biomaterials 108:3045–3055. 10.1002/jbm.b.34633
14. Sun TW, Yu WL, Qi C, Chen F, Zhu YJ, He YH (2017) Multifunctional simvastatin-loaded porous hydroxyapatite microspheres/collagen composite scaffold for sustained drug release, angiogenesis and osteogenesis. J Controlled Release 259:E130–E130. 10.1016/j.jconrel.2017.03.266
15. Xie PS, Zhang JH, Wu PF, Wu YJ, Hong YJ, Wang JN, Cai ZW (2023) Multicellular tumor spheroids bridge the gap between two-dimensional cancer cells and solid tumors: The role of lipid metabolism and distribution. Chinese Chemical Letters 34. doi: ARTN 10734910.1016/j.cclet.2022.03.072
16. Lee SI, Choi YY, Kang SG, Kim TH, Choi JW, Kim YJ, Kim TH, Kang T, Chung BG (2022) 3D Multicellular Tumor Spheroids in a Microfluidic Droplet System for Investigation of Drug Resistance. Polymers 14. doi: ARTN 375210.3390/polym14183752
17. Arora L, Kalia M, Roy S, Pal D (2022) Assessment of Mitochondrial Health in Cancer-Associated Fibroblasts Isolated from 3D Multicellular Lung Tumor Spheroids. Jove-Journal of Visualized Experiments doi: ARTN e6431510.3791/64315
18. Teufelsbauer M, Rath B, Plangger A, Staud C, Nanobashvili J, Huk I, Neumayer C, Hamilton G, Radtke C (2020) Effects of metformin on adipose-derived stromal cell (ADSC) - Breast cancer cell lines interaction. Life Sciences 261. doi: ARTN 11837110.1016/j.lfs.2020.118371
19. Ali NM, Yeap SK, Ho WY, Boo L, Ky H, Satharasinghe DA, Tan SW, Cheong SK, Huang HD, Lan KC, Chiew MY, Ong HK (2021) Adipose MSCs Suppress MCF7 and MDA-MB-231 Breast Cancer Metastasis and EMT Pathways Leading to Dormancy via Exosomal-miRNAs Following Co-Culture Interaction. Pharmaceuticals 14. doi: ARTN 810.3390/ph14010008
20. Wang Y, Chu YJ, Ren XF, Xiang HF, Xi YM, Ma XX, Zhu K, Guo Z, Zhou CL, Zhang GQ, Chen BH (2019) Epidural adipose tissue-derived mesenchymal stem cell activation induced by lung cancer cells promotes malignancy and EMT of lung cancer. Stem Cell Research & Therapy 10. doi: ARTN 16810.1186/s13287-019-1280-3
21. Song Y, Peng CL, Lv SS, Cheng J, Liu SS, Wen Q, Guan GJ, Liu G (2017) Adipose-derived stem cells ameliorate renal interstitial fibrosis through inhibition of EMT and inflammatory response via TGF-beta 1 signaling pathway. Int Immunopharmacol 44:115–122. 10.1016/j.intimp.2017.01.008
22. Xie J, Shen K, Lenchine RV, Gethings LA, Trim PJ, Snel MF, Zhou Y, Kenney JW, Kamei M, Kochetkova M, Wang X, Proud CG (2018) Eukaryotic elongation factor 2 kinase upregulates the expression of proteins implicated in cell migration and cancer cell metastasis. Int J Cancer 142:1865–1877. 10.1002/ijc.31210
23. Wu Q, Hu Q, Hai Y, Li Y, Gao Y (2023) METTL13 facilitates cell growth and metastasis in gastric cancer via an eEF1A/HN1L positive feedback circuit. J Cell Commun Signal 17:121–135. 10.1007/s12079-022-00687-x
24. Park YM, Yoo SH, Kim SH (2013) Adipose-derived stem cells induced EMT-like changes in H358 lung cancer cells. Anticancer Res 33:4421–4430
25. Chen D, Liu S, Ma H, Liang X, Ma H, Yan X, Yang B, Wei J, Liu X (2015) Paracrine factors from adipose-mesenchymal stem cells enhance metastatic capacity through Wnt signaling pathway in a colon cancer cell co-culture model. Cancer Cell Int 15:42. 10.1186/s12935-015-0198-9
26. Osugi Y, Fumoto K, Kikuchi A (2019) CKAP4 Regulates Cell Migration via the Interaction with and Recycling of Integrin. Mol Cell Biol 39. 10.1128/MCB.00073-19

27. Erdogan B, Ao M, White LM, Means AL, Brewer BM, Yang L, Washington MK, Shi C, Franco OE, Weaver AM, Hayward SW, Li D, Webb DJ (2017) Cancer-associated fibroblasts promote directional cancer cell migration by aligning fibronectin. J Cell Biol 216:3799–3816. 10.1083/jcb.201704053
28. Sigorski D, Wesolowski W, Gruszecka A, Gulczynski J, Zielinski P, Misiukiewicz S, Kitlinska J, Izycka-Swieszewska E (2023) Neuropeptide Y and its receptors in prostate cancer: associations with cancer invasiveness and perineural spread. J Cancer Res Clin Oncol 149:5803–5822. 10.1007/s00432-022-04540-x
29. Campos DFD, Marquez AB, O'Seanain C, Fischer H, Blaeser A, Vogt M, Corallo D, Aveic S (2019) Exploring Cancer Cell Behavior In Vitro in Three-Dimensional Multicellular Bioprintable Collagen-Based Hydrogels. Cancers 11. doi: ARTN 18010.3390/cancers11020180
30. Magdeldin T, Lopez-Davila V, Villemant C, Cameron G, Drake R, Cheema U, Loizidou M (2014) The efficacy of cetuximab in a tissue-engineered three-dimensional in vitro model of colorectal cancer. J Tissue Eng 5:2041731414544183. 10.1177/2041731414544183
31. Harper E, Agadi E, Sheedy E, Carey P, Wilkinson P, Siroky M, Hilliard T, Low E, Leonard A, Liu YY, Yang J, Stack MS (2022) Age-related changes in microenvironmental collagen affect ovarian cancer metastasis. Cancer Res 82
32. Chen DX, Liu ZYZ, Liu WJ, Fu MT, Jiang W, Xu SY, Wang GX, Chen F, Lu JP, Chen H, Dong XY, Li GX, Chen G, Zhuo SM, Yan J (2021) Predicting postoperative peritoneal metastasis in gastric cancer with serosal invasion using a collagen nomogram. Nature Communications 12. doi: ARTN 17910.1038/s41467-020-20429-0
33. Chen W, Park S, Patel C, Bai YX, Henary K, Raha A, Mohammadi S, You LD, Geng F (2021) The migration of metastatic breast cancer cells is regulated by matrix stiffness via YAP signalling. Heliyon 7. doi: ARTN e0625210.1016/j.heliyon.2021.e06252
34. Blyth RRR, Birts CN, Beers SA (2023) The role of three-dimensional in vitro models in modelling the inflammatory microenvironment associated with obesity in breast cancer. Breast Cancer Res 25:104. 10.1186/s13058-023-01700-w
35. Wang YY, Hung AC, Wu YC, Lo S, Chen HD, Chen YK, Hsieh YC, Hu SC, Hou MF, Yuan SF (2022) ADSCs stimulated by resistin promote breast cancer cell malignancy via CXCL5 in a breast cancer coculture model. Sci Rep 12:15437. 10.1038/s41598-022-19290-6
36. Lee SH, Cheng H, Yuan Y, Wu S (2014) Regulation of ionizing radiation-induced adhesion of breast cancer cells to fibronectin by alpha5beta1 integrin. Radiat Res 181:650–658. 10.1667/RR13543.1
37. Varadaraj A, Jenkins LM, Singh P, Chanda A, Snider J, Lee NY, Amsalem-Zafran AR, Ehrlich M, Henis YI, Mythreye K (2017) TGF-beta triggers rapid fibrillogenesis via a novel TbetaRII-dependent fibronectin-trafficking mechanism. Mol Biol Cell 28:1195–1207. 10.1091/mbc.E16-08-0601
38. Ahmed KM, Zhang H, Park CC (2013) NF-kappaB regulates radioresistance mediated by beta1-integrin in three-dimensional culture of breast cancer cells. Cancer Res 73:3737–3748. 10.1158/0008-5472.CAN-12-3537

Scheme

Scheme 1 is available in the Supplementary Files section

Figures

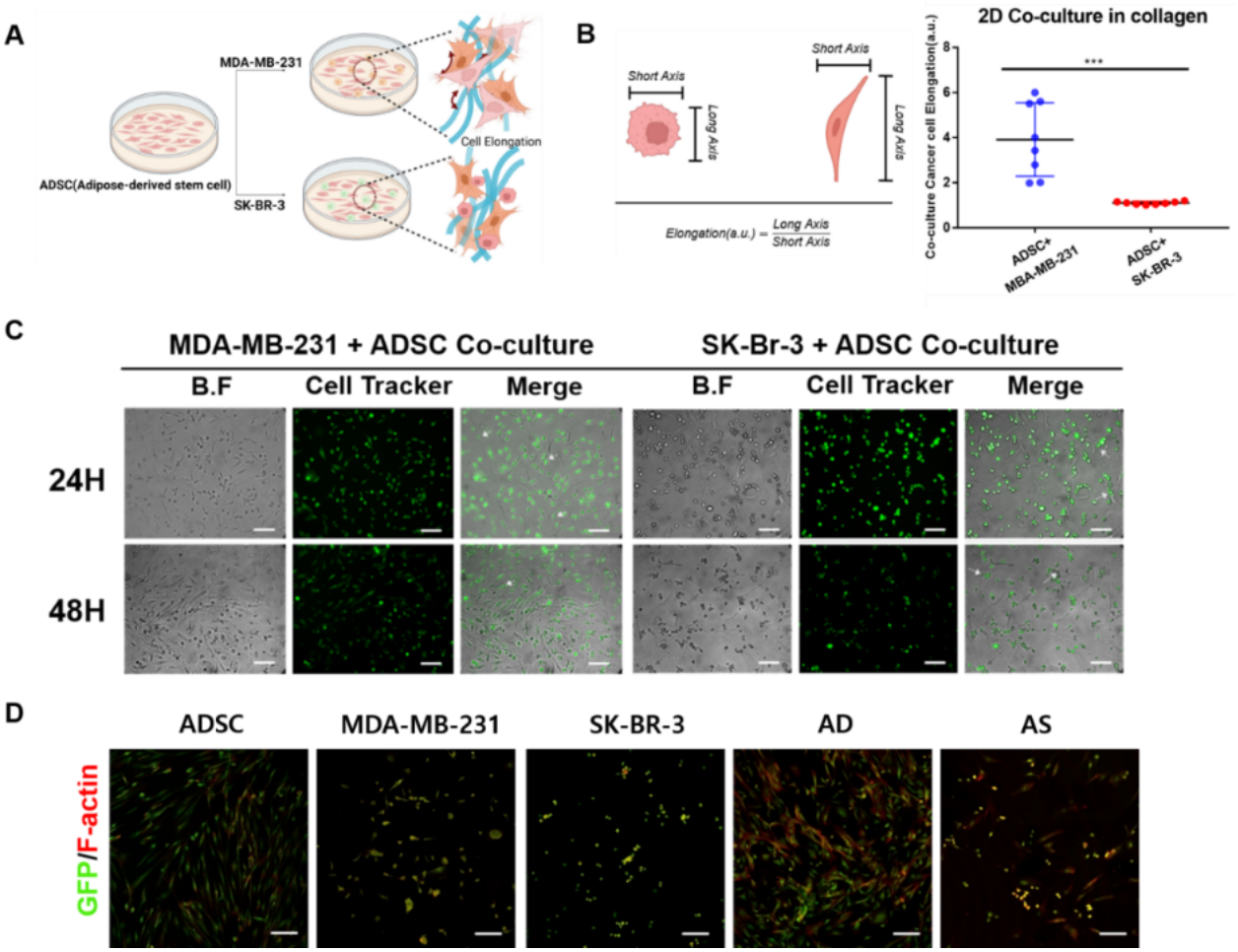

Figure 1

(a) Schematic illustration of the 2D co-culture system of adipose-derived stem cells (ADSCs) and breast cancer cell lines (MDA-MB-231 and SK-BR-3) in a collagen matrix. (b) Quantification analysis of cell elongation, breast cancer cells, and ADSCs in a co-cultured condition (n = 7). (c) Cell elongation observation of the 2D co-culture of ADSCs and breast cancer cell lines in a collagen matrix by using a cell tracker (scale bar: 500 μm). (d) Immunofluorescence of green fluorescent protein and F-actin for staining ADSCs only and ADSCs co-cultured with the breast cancer cells. (scale bar: 500 μm) (data are presented as the mean ± SEM; p value: ***p < 0.001).

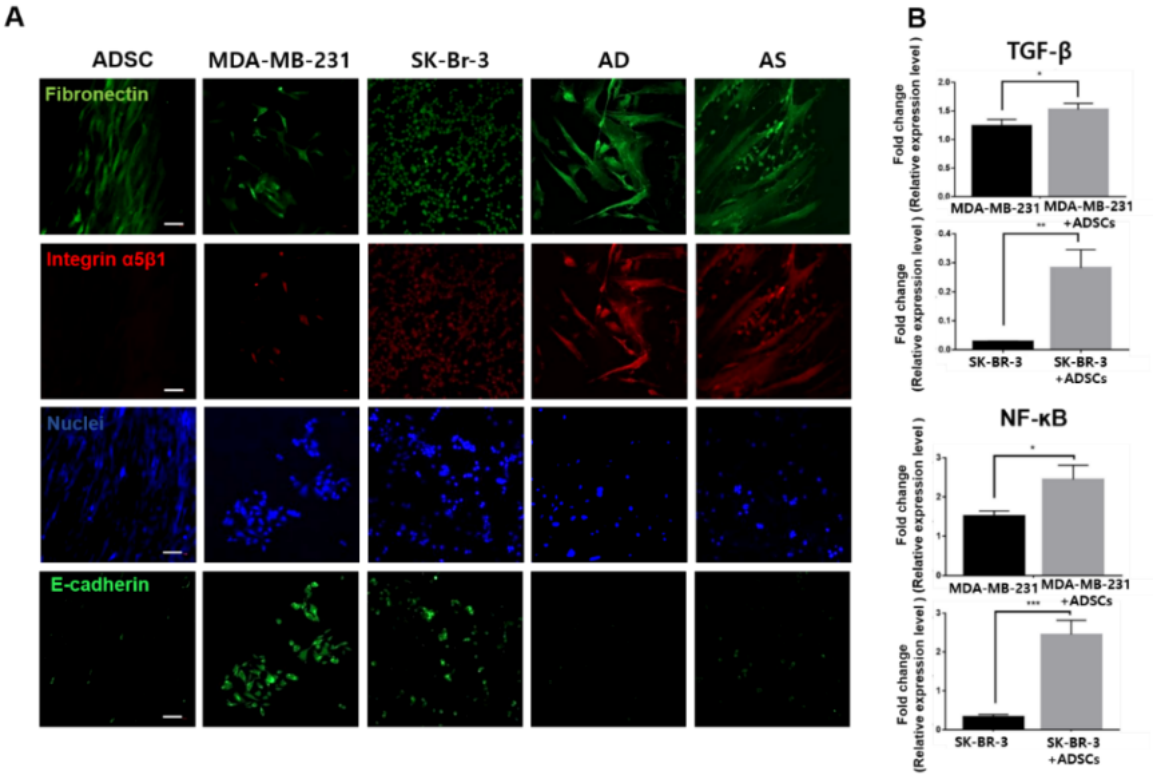

Figure 2

(a) Immunofluorescence image of 2D cancer monoculture and ADSC and breast cancer cell co-culture. (b) RT-qPCR for the gene expression of breast cancer cells only and co-culture with ADSCs (scale bar: 500 mm) (n = 3). Data are presented as the mean ± SEM; p values: $p < 0.05$, $^{**}p < 0.01$, and $^{***}p < 0.001$).

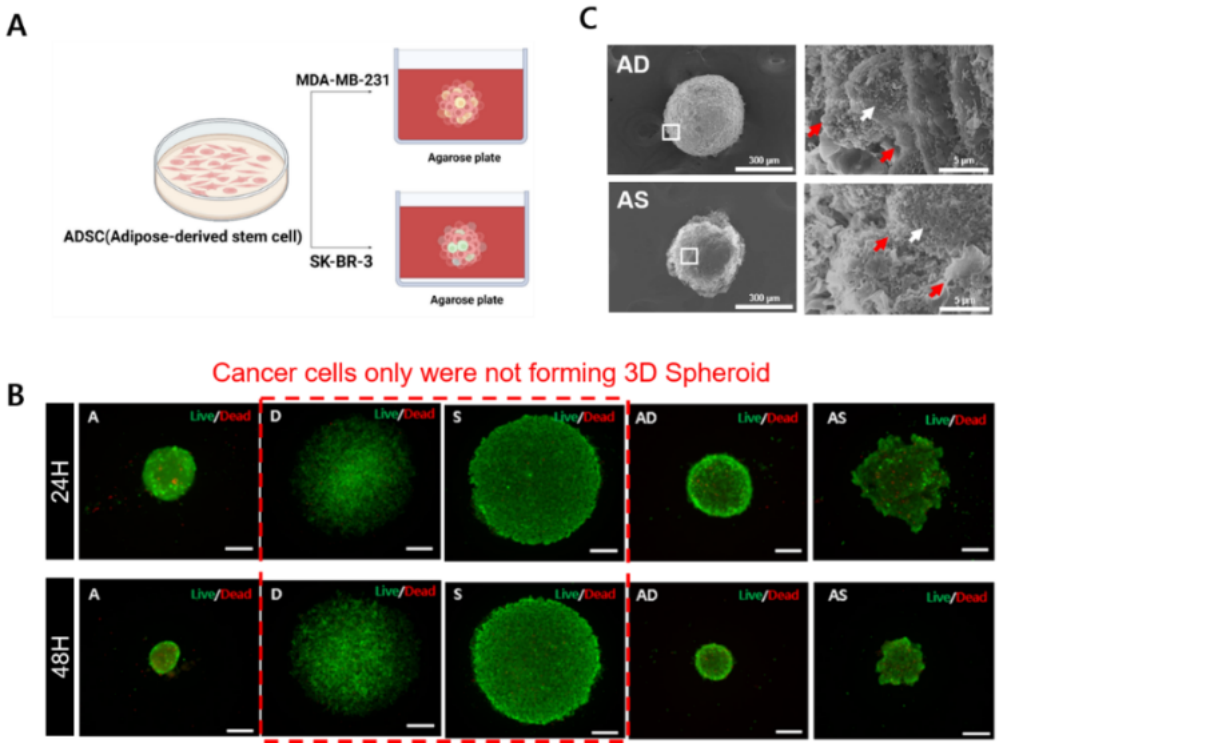

Figure 3

(a) Schematic illustration of 3D co-culture spheroid platform of the ADSCs and breast cancer cells (MDA-MB-231 and SK-BR-3) in a collagen matrix. (b) Live/dead image of 3D spheroid monocultures of ADSCs, MDA-MB-231, and SK-BR-3 and the ADSCs and MDA-MB-231 and ADSCs and SK-BR-3 co-culture groups for observing cell cytotoxicity for 24 and 48 hours each. The monocultures of MDA-MB-231 and SK-BR-3 did not form a spheroid. (A: ADSCs, D: MDA-MB-231, S: SK-BR-3, AD: ADSC and MDA-MB-231, AS: ADSC and SK-BR-3) (scale bar: 500 μm). (c) Scanning electron image of 3D spheroid ADSC and MDA-

MB-231 and ADSC and SK-BR-3. The red arrow indicates the shape of the ECM fibers on the cell surfaces, and white arrow indicates the breast cancer cells (scale bar: 300 and 5 μm, respectively).

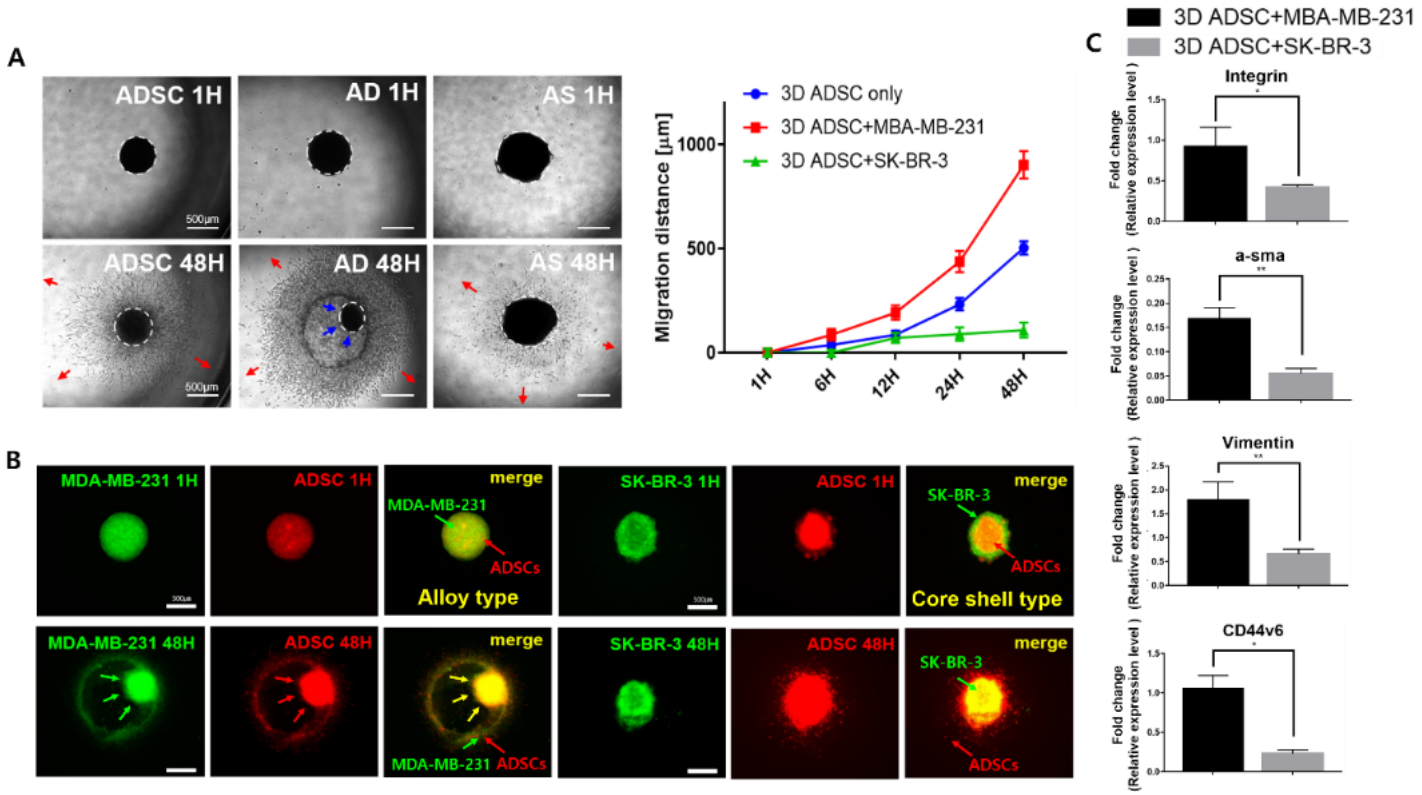

Figure 4

(a) Bright-field image of the migration of 3D spheroid adipose-derived stem cells (ADSCs) only and the ADSC+MDA-MB-231 (AD) and ADSC+SK-BR-3 (AS) groups (red arrow: migrated cells [scale bar: 500 μm], blue arrow: cell aggregation). The graph illustrates their migration distance (migration distance = migrated cell distance– spheroid radius [1 hour], n = 10). (b) Fluorescence image of the 3D spheroid migration profile. The breast cancer cells were stained using Green cell tracker, while the ADSCs were stained using Vybrant dye (green arrow: breast cancer cells, red arrow: ADSCs; scale bar: 500 μm). (c) Gene relative expression level of the AD and AS groups. (n = 3, data are represented as the mean ± SEM; p values: *p < 0.05, **p < 0.01, and ***p < 0.001).

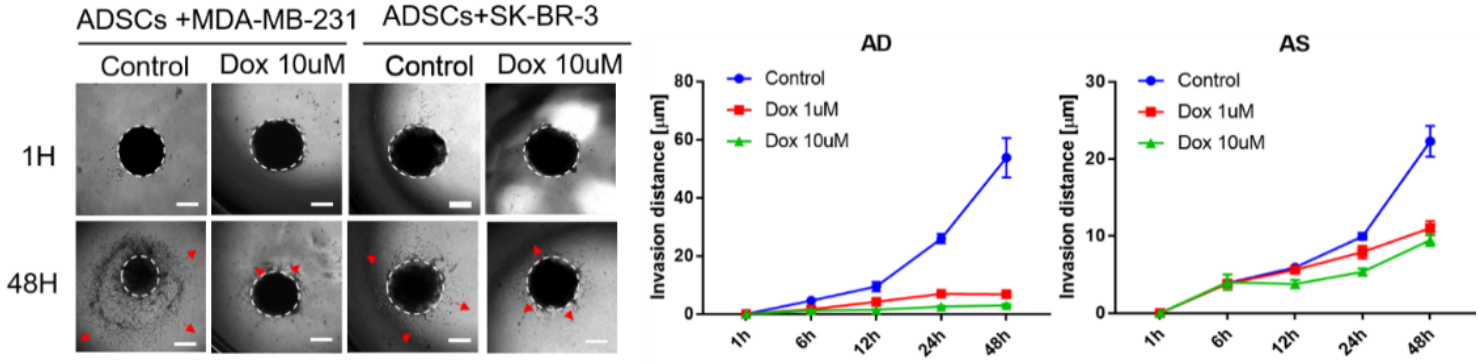

Figure 5

Image shows the migration test after treating the ADSCs+MDA-MB-231 (AD) and ADSCs+SK-BR-3 (AS) groups with doxorubicin (1 and 48 hours) (scale bar: 500 μm). The red arrow indicates the spreading of cells. Graph illustrates the invasion distance (μm) between the AD and AS groups after doxorubicin treatment at 1 and 10 μM concentrations, respectively (n = 10, data are presented as the mean ± SEM).

Supplementary Files

This is a list of supplementary files associated with this preprint. Click to download.

- Supplementarymaterial.docx
- floatimage1.png